SCIENTIFIC REPORTS

OPEN

SUBJECT AREAS:
SECRETION
FUNGAL GENOMICS
FUNGAL BIOLOGY

Received
29 September 2014

Accepted
12 December 2014

Published
14 January 2015

Correspondence and requests for materials should be addressed to L.R.A. (lysalves@fiocruz.br)

Extracellular vesicle-mediated export of fungal RNA

Roberta Peres da Silva[1], Rosana Puccia[1], Marcio L. Rodrigues[2,3], Débora L. Oliveira[3], Luna S. Joffe[2], Gabriele V. César[3], Leonardo Nimrichter[3], Samuel Goldenberg[4] & Lysangela R. Alves[4]

[1]Departamento de Microbiologia, Imunologia e Parasitologia da Escola Paulista de Medicina-UNIFESP, São Paulo, SP, Brazil, [2]Centro de Desenvolvimento Tecnológico em Saúde (CDTS), Fundação Oswaldo Cruz, Rio de Janeiro, RJ, Brazil, [3]Instituto de Microbiologia Professor Paulo de Góes, Universidade Federal do Rio de Janeiro, Rio de Janeiro, RJ, Brazil, [4]Instituto Carlos Chagas, Fundação Oswaldo Cruz, Fiocruz-PR, Curitiba, PR, Brazil.

Extracellular vesicles (EVs) play an important role in the biology of various organisms, including fungi, in which they are required for the trafficking of molecules across the cell wall. Fungal EVs contain a complex combination of macromolecules, including proteins, lipids and glycans. In this work, we aimed to describe and characterize RNA in EV preparations from the human pathogens *Cryptococcus neoformans*, *Paracoccidiodes brasiliensis* and *Candida albicans*, and from the model yeast *Saccharomyces cerevisiae*. The EV RNA content consisted mostly of molecules less than 250 nt long and the reads obtained aligned with intergenic and intronic regions or specific positions within the mRNA. We identified 114 ncRNAs, among them, six small nucleolar (snoRNA), two small nuclear (snRNA), two ribosomal (rRNA) and one transfer (tRNA) common to all the species considered, together with 20 sequences with features consistent with miRNAs. We also observed some copurified mRNAs, as suggested by reads covering entire transcripts, including those involved in vesicle-mediated transport and metabolic pathways. We characterized for the first time RNA molecules present in EVs produced by fungi. Our results suggest that RNA-containing vesicles may be determinant for various biological processes, including cell communication and pathogenesis.

The extracellular release of macromolecules is essential for a number of physiological events in fungal cells, including nutrition, intercellular communication, biofilm formation and, in pathogenic fungi, activation of immune cells[1,2]. Fungal cells are encased within a dense cell wall, so mechanisms are required for the transport of molecules across the wall for extracellular release in these organisms. In recent years, a number of studies have shown that the trafficking of molecules across the fungal cell wall requires extracellular vesicles (EVs)[3–18].

Fungal EVs contain a complex combination of macromolecules, including many proteins, neutral lipids, glycans and pigments[3,4,7,9,10,14,15,18]. This complex molecular mixture, including many cytoplasmic components, is consistent with the proposed origin of fungal EVs as cytoplasmic subtractions[19]. This would suggest that the complexity of the composition of fungal EVs may be underestimated, because it is not possible to rule out the presence of other macromolecules present in the cytoplasm.

Fungal and mammalian EVs have similar morphological features and compositions[20]. Mammalian EVs efficiently transport mRNA and other macromolecules to the extracellular space[1]. Interestingly, mRNAs from mammalian EVs can be translated into proteins by target cells[21,22]. It has recently been shown that EVs also contain small noncoding RNA species[22,23]. EV-associated RNA produced by pathogens could affect the physiology of host cells, as suggested by experiments with mammalian EV RNA[24,25].

The presence of RNA in fungal EVs was suggested by the findings of a single flow-cytometry study focusing on the human pathogen *Cryptococcus neoformans*[6]. However, the structural aspects of EV-associated fungal RNA remain to be explored. In this study, we selected four species of EV-producing fungal cells for an analysis of the presence of RNA sequences. Our results for the model yeast *Saccharomyces cerevisiae* and the human pathogens *C. neoformans, Paracoccidioides brasiliensis*, and *Candida albicans*, demonstrated that fungal cells use EVs to export RNA molecules of different natures and with different biological functions.

Results and Discussion

Comparative transcriptomic analysis of fungal extracellular vesicles (EVs). Total RNA was isolated from fungal EVs in three independent biological replicates. The RNA was then fractionated into samples enriched

in small RNAs (less than 200 bp) and mRNAs. The small RNA-enriched fractions were then analyzed, to determine their molecular size distribution (Fig. 1A). EV small-RNA fractions consisted of molecules of various sizes, mostly fewer than 250 nucleotides long. One preparation obtained from *P. brasiliensis* Pb18 illustrate this profile (Fig. 1A), and similar observations were made for all the species studied. We conclude that fungal EVs carry small RNA molecules with similar size distributions.

We checked that RNA molecules were not loosely aggregated with fungal EV rather than being packaged within these vesicles, by subjecting control samples to RNAse treatment before RNA extraction (Fig. 1B). The small-RNA profile of RNAse-treated EVs was not modified, confirming that the small RNA molecules were within the vesicles, which protected them from hydrolysis. We also assessed RNase activity, by adding exogenous, total fungal RNA EV preparations before RNase treatment. The total RNA was degraded, consistent with functional RNase-mediated hydrolysis (Fig. S1A to D).

Genome RNA EV mapping statistics are listed in Table 1. For *C. neoformans* samples, about 90% of the RNA EV reads mapped to intronic regions, the remaining 10% mapping to exons, in mature mRNA. A similar profile was clearly observed in *P. brasiliensis* samples, in which 17% of the reads mapped to intronic regions and 82% mapped to exons. However, 21% of the reads in *P. brasiliensis* mapped to exon-intron regions, versus less than 1% of the mapped reads in *C. neoformans*. In *S. cerevisiae* and *C. albicans*, about 90% of the reads mapped to exons. This observation is consistent with the introns lower number in these species[26,27], by contrast to *P. brasiliensis* and *C. neoformans*.

Gemome RNA EV mapping information is illustrated in Figure 2. Reads mapping to an entire mRNA (Fig. 2A), intergenic (Fig. 2B) and intronic regions (Fig. 2C), or aligning with specific positions in the

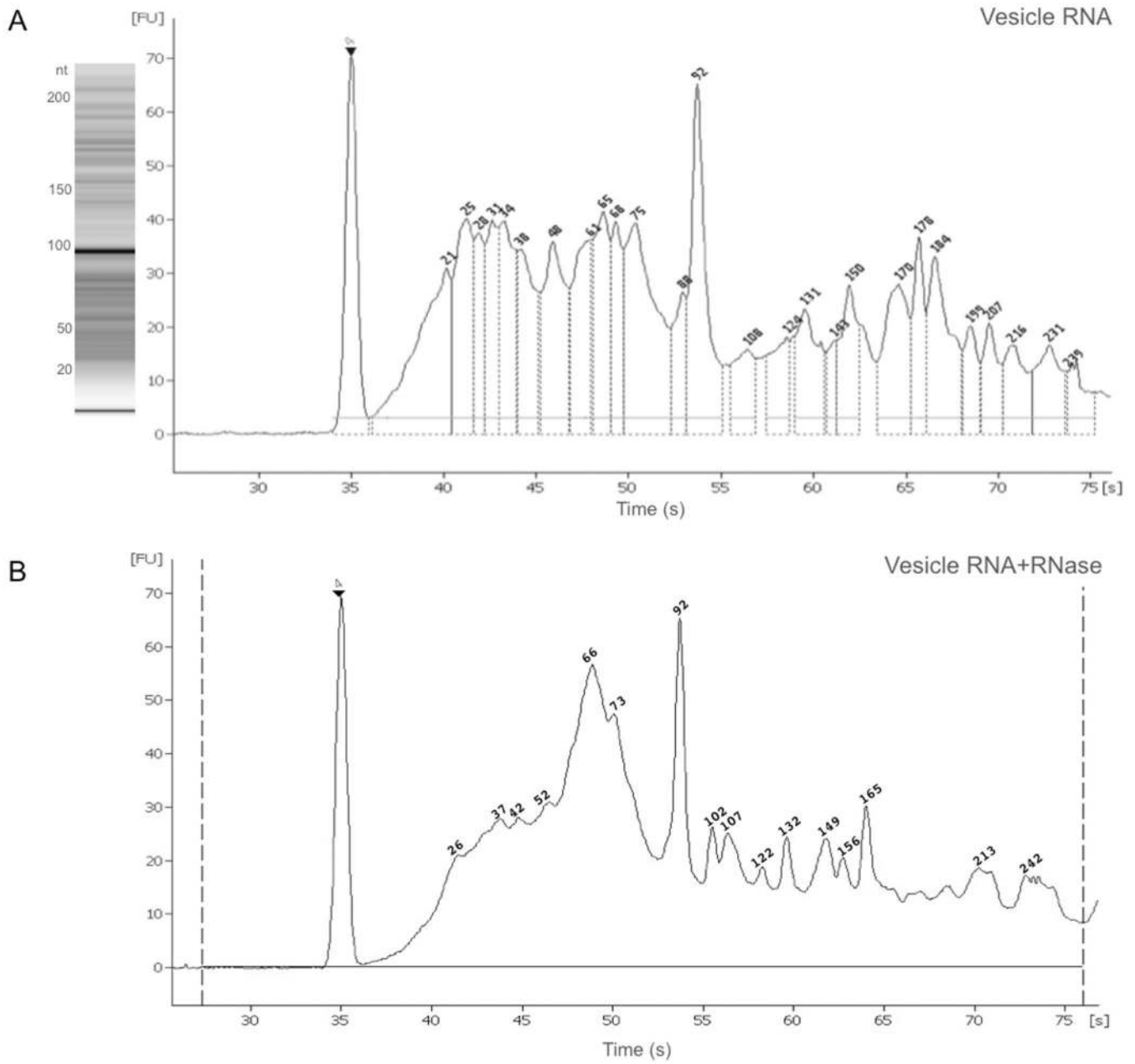

Figure 1 | Electropherograms of the small-RNA content of EVs from the Pb18 strain of *P. brasiliensis* (A) and the control with RNAse treatment (B). Retention time (s) and fluorescence intensity (FU) are indicated on the corresponding axes of the graphs generated from the profiles shown on the left. RNA length (bp) is shown for each peak.

Table 1 | Sequence mapping statistics

	C. neoformans		*C. albicans*		*P. brasiliensis*		*S. cerevisiae*	
	Uniquely mapped	% of total mapped	Uniquely mapped	% of total mapped	Uniquely mapped	% of total mapped	Uniquely mapped	% of total mapped
Exon-exon	5029.5	0.4	43	0	2395	1.4	234.3	0.1
Exon-intron	10664	0.6	33	0	40110	21.9	118.3	0
Total exon	113654.5	9.7	267230	93.9	136730	82.4	327028	84.6
Total intron	1003971	90.3	13853	6.1	25965	17.6	36170.3	15.4
Total gene	1117625	100	281083	100	162695	100	363198.3	100

mRNA (Fig. 2D) were observed for all species studied. This suggests that, in addition to the small RNA molecules previously observed, mRNAs are also present in fungal EVs. Most of the reads aligning with intergenic and intronic regions were found to be in the reverse orientation, complementary to the transcript (Fig. 2D). This pattern is characteristic of sequences processed by the small-RNA interference (RNAi) machinery[28,29].

Small RNA characterization: miRNA-like sequences. For the identification of conserved miRNA sequences among the small RNAs identified in EVs from *P. brasiliensis*, *C. neoformans*, *C. albicans*, and *S. cerevisiae*, we used a database of mature miRNA sequences from all organisms characterized to date (http://www.mirbase.org/). We identified a total of 1,246 conserved miRNA-like sequences, only 20 of which were common to all four fungal species studied (Table 2). The total numbers of miRNAs identified were 145 (1,953 mean reads) for *P. brasiliensis*, 344 (4,796 mean reads) for *C. neoformans*, 423 (2,477 mean reads) for *C. albicans*, and 532 (4,349 mean reads) for *S. cerevisiae* (Table S1). We then used Baggerly's test[30] to compare the levels of miRNA-like molecules in EVs among the four species. We found that 47 of these molecules were differentially distributed (Fig. 3). *C. neoformans* had the largest number of overrepresented sequences (16), followed by *C. albicans* (8), *P. brasiliensis* (12), and *S. cerevisiae* (1). We also identified five miRNA-like sequences exclusive to *P. brasiliensis* and one exclusive to *S. cerevisiae*. The distribution of miRNA-like molecules was more similar in *C. neoformans* and *C. albicans* EV, although the values for *C. neoformans* were considerably higher for most sequences (Fig. 3).

Emu-miR-8, egr-miR-8, tae-miR-156, osa-miR-156f, and ata-miR-172f were more frequently represented in *C. neoformans* and *C. albicans* (Fig. 3). Members of these miRNA families are involved in the development of *Drosophila*[31–33], zebrafish[34], tumors[35], and plants[36]. Sequences pvu-miR166a and ssl-miR166a, involved in plant biology[37,38], were identified in *P. brasiliensis*, *C. neoformans*, and *S. cerevisiae*.

Five miRNA-like sequences were exclusive to *P. brasiliensis* EVs (Fig. 3). One of them, dre-miR 125a-2, belongs to the miR 125 family, which is highly conserved in eukaryotes[39] and is involved in many different cellular processes, including cell proliferation[40,41], differentiation and apoptosis, through the targeting of different transcription factors[40], matrix-metalloproteases[42,43], growth factors[44] and nonsense-mediated mRNA decay pathway[45]. In addition, miR-125 controls the differentiation of immune cells, thereby affecting responses to bacterial and viral infection[39,46–49].

Many fungal species have RNAi machinery, which may be non-canonical in *Schizosaccharomyces pombe*, for e.g., or absent from others (e.g. *S. cerevisiae*), and functional in most filamentous fungi[50–53]. *C. neoformans* bears a fully functional RNAi machinery,

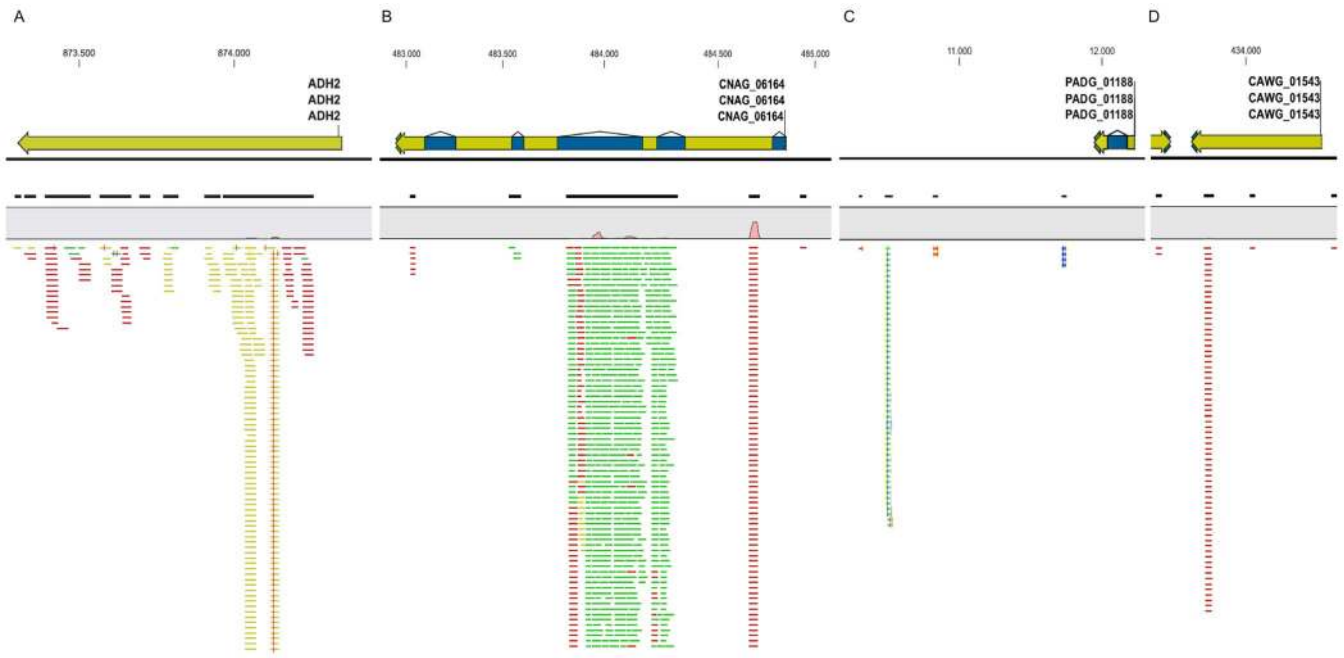

Figure 2 | Genome RNA EVs mapping (A), high-coverage exon; (B) intron; (C), intergenic regions; (D) low-coverage exon. Gray bar, genomic region, with length in bp, shown above; black lines above the reads, consensus; vertical columns, number of sequences; yellow bars, exons (access codes shown); blue bars, introns. For the sequence colors: forward reads, red; reverse reads, green and non-specific match, yellow.

Table 2 | miRNA-like common sequences from *P. brasiliensis*, *C. neoformans*, *C. albicans*, and *S. cerevisiae* EVs. Means of normalized values are shown

Feature ID	*C. albicans*	*C. neoformans*	*P. brasiliensis*	*S. cerevisiae*
Aau-MIR172	118.37	732.16	217.01	17.58
aly-MIR159c	353.98	1852.68	434.03	116.95
aly-MIR408	707.96	905.99	840.84	8.79
ata-MIR172	3643.60	2667.29	1369.77	512.57
cin-mir-4000c	3539.19	961.54	217.01	108.15
cre-MIR909	101.07	133.12	623.83	116.95
cre-MIR916	8351.86	4633.87	311.92	604.06
gma-MIR408b	1181.44	2107.91	434.03	76.93
mmu-mir-5102	15297.93	8184.08	217.01	6716.77
mmu-mir-5110	1230.16	1923.08	311.92	116.95
osa-MIR156f	1805.63	3494.66	623.83	935.94
osa-MIR408	202.14	1172.23	311.92	125.74
peu-MIR2916	2899.44	3110.15	1871.49	12065.74
pta-MIR1310	293384.35	116870.19	153791.50	147045.22
pvu-MIR166a	118.37	2536.97	311.92	610.65
sbi-MIR396c	1314.85	13800.48	651.04	316.95
sha-mir-716a	91615.15	126265.66	2699.07	47842.09
sha-mir-716b	168637.59	326375.49	642856.87	665774.04
sme-mir-2152	51962.07	110498.84	528.93	4609.00
smo-MIR1082a	1267.48	20639.54	31127.89	356.52

including Argonaute proteins, Dicer and the RNA-dependent RNA polymerase[54,55]. In this organism, RNAi-dependent mechanisms are involved in the sex-induced silencing of transgenes during the sexual stage of the fungus[55]. In addition, *C. neoformans* miRNA and pre-miRNA may be similar to their mammalian counterparts[54,55]. In *C. albicans*, the RNAi machinery includes a noncanonical Dicer, and small-RNA molecule preparations from this species are enriched in 22-mer sequences[56]. The occurrence of RNAi machineries in different fungal pathogens suggests a possible role for miRNA-like molecules during with the interaction of fungi with their host cells, possibly involving the mimicking of endogenous miRNA. This putative mechanism might regulate gene expression in host cells and modify sensitivity to infection. Further investigations, determining the roles of small RNAs in fungal EVs, are required to test this hypothesis.

Identification of non-coding RNAs (ncRNAs). Our analysis of RNA sequences in fungal EVs included classes of non-coding RNA other than miRNAs. These classes were identified with the use of ncRNA data from the *Saccharomyces* Genome Database as a template. We identified a total of 114 different ncRNA sequences in EV preparations, many of which were specifically associated with *C. neoformans* (46), *P. brasiliensis* (38), *C. albicans* (68), or *S. cerevisiae* (106). Eleven ncRNAs were common to all four fungal species (Table 3 and Table S2): one tRNA, two snRNAs, two rRNAs and six snoRNAs. None of the roles of these ncRNAs had previously been characterized during host-parasite interactions.

The ncRNA groups most frequently represented in all fungal EV preparations were small nucleolar RNAs (snoRNAs) and tRNAs, which accounted for 22 to 75% of all reads (Fig. 4). *S. cerevisiae* had a high proportion of snoRNA (75%), whereas tRNAs accounted for 60% of all reads in *C. albicans*. In *C. neoformans*, for the most part, reads were fairly evenly distributed between snoRNAs and tRNAs. *P. brasiliensis* had a slightly different profile, with long ncRNAs accounting for 8% of the sequences and rRNAs accounting for 13%.

Only eight long ncRNA species were identified in our samples (Table S2). None was common to all fungal EVs, but most were identified in at least two species. In mammalian cells, the transcription of several long ncRNAs is regulated by factors critical for mammalian development[57–60]. This suggests possible key roles in development for these ncRNAs, through the regulation of protein synthesis by mechanisms independent of the Dicer RNAi pathway[57,60]. Table S2 highlights the involvement of ICR1[57], a *cis*-interfering long intergenic ncRNA that regulates transcription of the *FLO11* locus in *S. cerevisiae*. ICR1 and PWR1 form a circuit with a bidirectional toggle, including the upstream signaling pathway transcription factors Sfl1 and Flo8, and the chromatin remodeler Rpd3L, which is essential for phenotypic transitions in yeast[57,60].

The ncRNA RPR1 was identified in *S. cerevisiae* EV samples. It interacts with nine other proteins to form the ribonuclease P (RNase P) complex, a ubiquitous endoribonuclease that cleaves precursor tRNAs to generate mature 5' termini[61]. RNase P is also involved in the turnover of normally unstable nuclear RNA[62]. The RNA component of mitochondrial RNase P, RPM1[63], was found in EVs from three fungal species. Another component of a mitochondrial RNAse – NME1 – was found in EV samples from *C. albicans* and *S. cerevisiae*. NME1 is a subunit of the essential ribonucleoprotein endoribonuclease, RNase MRP, which is required for the processing of pre-rRNA. *In vitro*, it promotes the cleavage of pre-5.8S rRNA[64,65] and the degradation of specific mRNA sequences involved in cell cycle regulation[66].

snRNAs constitute a small group of highly abundant, non-polyadenylated ncRNA transcripts present in the nucleoplasm[67,68]. They form the core of the spliceosome and catalyze the removal of introns from pre-mRNA[67,68]. Four different snRNAs were found in fungal EVs (Table S2). LSR1 and snR19 were present in all species, snR6 was absent from *P. brasiliensis*, and snR14 was observed only in *C. albicans* and *S. cerevisiae*.

As mentioned above, 72 different snoRNA species were found in fungal EVs (Table S2). These RNAs can be classified into two groups on the basis of sequence motifs and secondary structures: C/D and H/ACA boxes, which are involved in the methylation and pseudouridylation of mammalian rRNA nucleotides, respectively[69]. They may also play a role in mRNA modification, participating in the control of expression[70]. The snoRNAs also guide rRNA nucleotide modifications and participate in pre-rRNA cleavage[71]. A few snoRNAs, such as snR10, have both functions. This molecule is required for normal cell growth, in addition to pre-rRNA processing in *S. cerevisiae*[72]. It was found in EVs from all species except *C. neoformans*. Other snoRNAs identified included U3 (SnR17a/b), U14 (SnR128), and snR30, which are essential for eukaryotic growth[73]. The collection of snoRNAs found in fungal EVs included snR191RNA, which has been reported to support cell growth in *S. cerevisiae*[74], whereas the snR70, snR71, SnR65, and SNR68 mutants display growth defects[75].

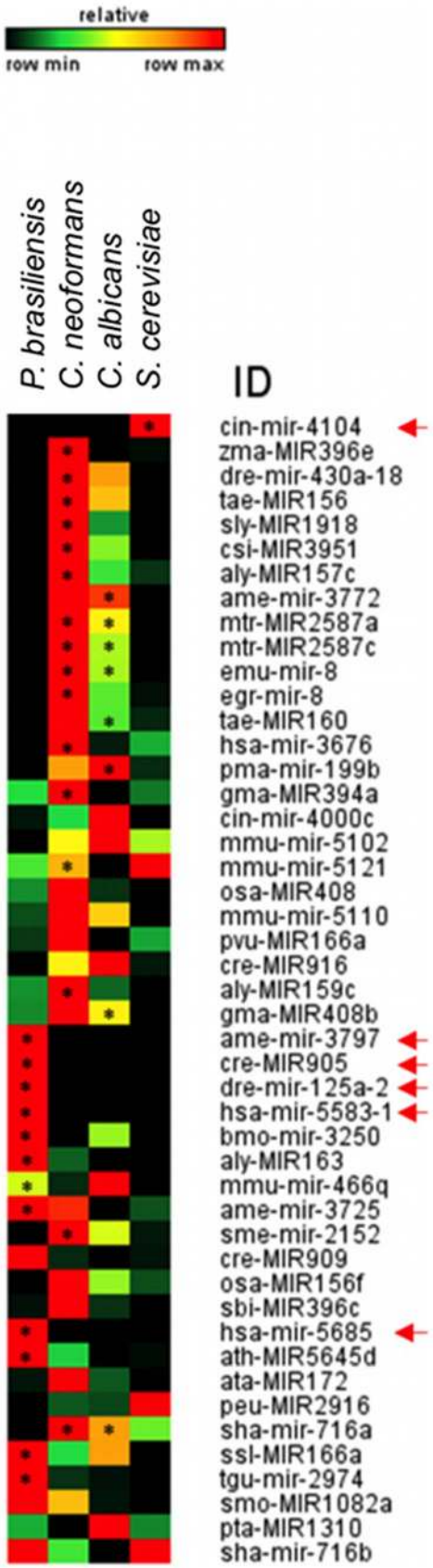

Figure 3 | Heat map of miRNA-like molecules showing relative levels in the EVs of *P. brasiliensis*, *C. neoformans*, *C. albicans*, and *S. cerevisiae*. All sequences with differential distributions between these species are shown. The colors on the plot depend on the replicate means of normalized miRNA-like sequence levels in the EVs of each of the fungal species. The highest value in each row is shown in red, and the other colors used change proportionally with the difference. *, the sequences most frequently represented in the species; arrows, unique sequences.

It is tempting to speculate that ncRNAs present in the *P. brasiliensis*, *C. neoformans*, *C. albicans*, and *S. cerevisiae* EV preparations may be involved in intercellular regulation, mostly through the regulation of protein synthesis.

The tRNAs constitute an interesting group of ncRNAs. The EVs of the fungal species studied containing 22 to 60% tRNAs, depending on the species analyzed (Fig. 5 and Table S2). In the protozoan parasite *Trypanosoma cruzi*, which has no RNAi machinery molecules, a PIWI-like protein has been characterized[76]. However, the cells of this parasite contain a homogeneous population of small RNAs derived from mature tRNAs, known as tsRNAs[77]. tsRNAs are produced by an alternative small RNA pathway[77]. Recent studies have shown that these molecules are packaged into vesicles that are shed by the parasite and can be transferred to other parasites and/or host cells[24,25]. The cargo of these vesicles can change the expression profile of the host cells, leading to changes in the cytoskeleton and extracellular matrix, increasing susceptibility to infection[24,25]. We detected fragments of mature tRNAs in the EVs of all the fungal species studied (Table 3 and Fig. 5). Fungal EVs were enriched in nuclear and mitochondrial tRNAs, which are not the most abundant population in the cell (Table 3). Specific enrichment in the 3′ region of the tsRNA was also observed (Fig. 5). This scenario is illustrated by the situation for arginine tRNA (CCU), which is present at a relatively low concentration in cellular compartments[78,79]. This tRNA, which was found in fungal EVs, is required for growth on nonfermentable carbon sources at high temperatures, for the synthesis of the heat shock protein Ssc1p, and for Ty1 retrotransposition, through the regulation of translational frameshift[78]. Our observations indicate that fungal EVs contain tsRNAs that might modify and affect gene expression in host cells.

mRNA identification. The sequencing of EV-associated small RNA-enriched fractions led to the identification of 253 different mRNAs in *C. albicans*, 84 in *S. cerevisiae*, 353 in *C. neoformans*, and 73 in *P. brasiliensis* (Table S3). The ten most abundant mRNAs from each species found are listed in Table 4. These sequences were obtained from high-coverage sRNAs (Fig. 1A), suggesting that molecules of more than 200 nt were copurified despite the use of a strategy favoring the purification of small RNAs. We validated the mRNA sequencing data obtained for fungal EVs, by performing RT-qPCR on two representative sequences corresponding to exons with and without high coverage rates (Fig. S2). The RNA-seq data demonstrated that the EV mRNA molecules corresponded to 1–2% of those found in intracellular compartments[26,27,80–82]. The most abundant EV mRNAs differed from the most abundant cellular transcripts, consistent with regulated compartmentalization for extracellular export. This observation is exemplified by the ASH1 mRNA from *S. cerevisiae*, which had an RPKM value of more than 200 in vesicles. This mRNA is not particularly frequent in total cellular mRNA, and is produced preferentially during cell budding[83]. Other examples include mRNAs required for the synthesis of the fatty acid desaturase Ole1, the heat-shock proteins Hsp104, Hsp82 and Hsp70, the regulator of endochitinase (CTS1) expression Nce2m, glyoxalate pathway regulators, a putative estradiol-binding protein, and a putative sterol transporter from *P. brasiliensis*. All these mRNAs are upregulated in yeast cells[81,84], but all were absent from EV preparations. The transcripts encoding urease and the cell division control protein CDC42, which may be involved in the pathogenicity of *P. brasiliensis*[81,84], were identified in the vesicles. In *C. albicans*, the most abundant vesicular mRNAs were the *CYB5* transcript (RPKM > 12,000), which encodes cytochrome *b*, and the *RTT109* transcript

Table 3 | ncRNA sequences identified in EV preparations from *C. neoformans* (Cn), *P. brasiliensis* (Pb), *S. cerevisiae* (Sc), and *C. albicans* (Ca)

RNA	Ca	Cn	Pb	Sc	Type	Function
15S_rRNA	X	X	X	X	rRNA mitochondrial	MSU1 allele suppresses ochre stop mutations in mitochondrial protein-coding genes
21S_rRNA	X	X	X	X		intron encodes the I-SceI DNA endonuclease
snR128	X	X	X	X	snoRNA	C/D box small nucleolar RNA
snR17a	X	X	X	X		small nucleolar RNA U3, part of Small ribosomal SubUnit (SSU) processosome
snR36	X	X	X	X		H/ACA box small nucleolar RNA
snR61	X	X	X	X		C/D box small nucleolar RNA
snR69	X	X	X	X		C/D box small nucleolar RNA
snR76	X	X	X	X		C/D box small nucleolar RNA
LSR1	X	X	X	X	snRNA	U2 spliceosomal RNA
snR19	X	X	X	X		U1 spliceosomal RNA
tR(CCU)J	X	X	X	X	tRNA	Arginine tRNA; low abundance tRNA required for growth on nonfermentable carbon sources

(RPKM > 3,500), encoding histone acetyltransferase. These transcripts are present at a relatively low abundance in *C. albicans* cells[85].

Gene ontology analysis revealed enrichment in RNA molecules relating to specific cellular processes in fungal EVs. Some of these processes, such as vesicle-mediated transport and metabolic pathways, were common to all four species analyzed in this study (Fig. 6). Other processes were limited to two species. For example, mycelium development and filamentous growth were restricted to *C. albicans* and *C. neoformans* (Fig. 6). Similarly, EV samples from *C. neoformans* and *P. brasiliensis* were enriched in mRNAs relating to cellular responses to stress, whereas those from *C. neoformans* and *S. cerevisiae* were rich in mRNAs involved in transcriptional regulation and those from *P. brasiliensis* and *S. cerevisiae* were enriched in mRNAs involved in cell cycle control (Fig. 6). These observations indicate that fungal EVs carry mRNAs common to different species, but they may also carry molecules restricted to one or two species. The biological significance of this finding is unknown.

We compared vesicular mRNA sequences from the four species studied, to identify sequences that were species-specific and characteristics common to EV preparations from *S. cerevisiae, C. neoformans, P. brasiliensis*, and *C. albicans*. In *C. neoformans*, the most abundant mRNAs with sequences corresponding to known functions (RPKM > 1,000) were those encoding citrate synthase, ubiquitin-activating enzyme, succinate dehydrogenase, VpsA (vacuolar protein sorting A), L7 ribosomal protein, ATP-binding cassette transporter, cellulase and the AGC/AKT protein kinase associated with the TOR complex. In *P. brasiliensis*, the most abundant transcripts with annotated functions corresponded to cell division control proteins, translation initiation factor RLI 1 and nucleotide-binding proteins. Most of the mRNAs identified in *C. albicans* encoded hypothetical proteins, but those encoding cytochrome b5, histone acetyltransferase, cell division control protein (CDC43) and arginine biosynthetic process 1 were also identified. Only three of the transcripts in *S. cerevisiae* samples had a RPKM value greater than 1,000; the most abundant mRNA were those encoding Myb-related transcription factor, the Dam-1 complex associated with cell division, a cyclin involved in cell cycle progression, a pheromone-regulated protein associated with mating, a component of autophagosomes, pre-mRNA splicing and inhibitor of HO transcription.

Many of the mRNA sequences found in EV preparations had a higher abundance than expected from genomic data (Table 5). For instance, in *S. cerevisiae*, vesicular mRNAs from the cellular protein modification process (2.18-fold) and small molecule metabolic process (1.82-fold) categories were more frequent than would be expected given the relative distribution of the corresponding genes in the genome (Table 1). Similar findings were obtained for the categories chromatin repression by histone regulators (5-fold) and mitosis regulator (2-fold) in *P. brasiliensis*. In *C. albicans*, vesicle samples were enriched in sequences required for vesicle-mediated transport (2.43-fold), catabolic processes (2.1-fold), and transport

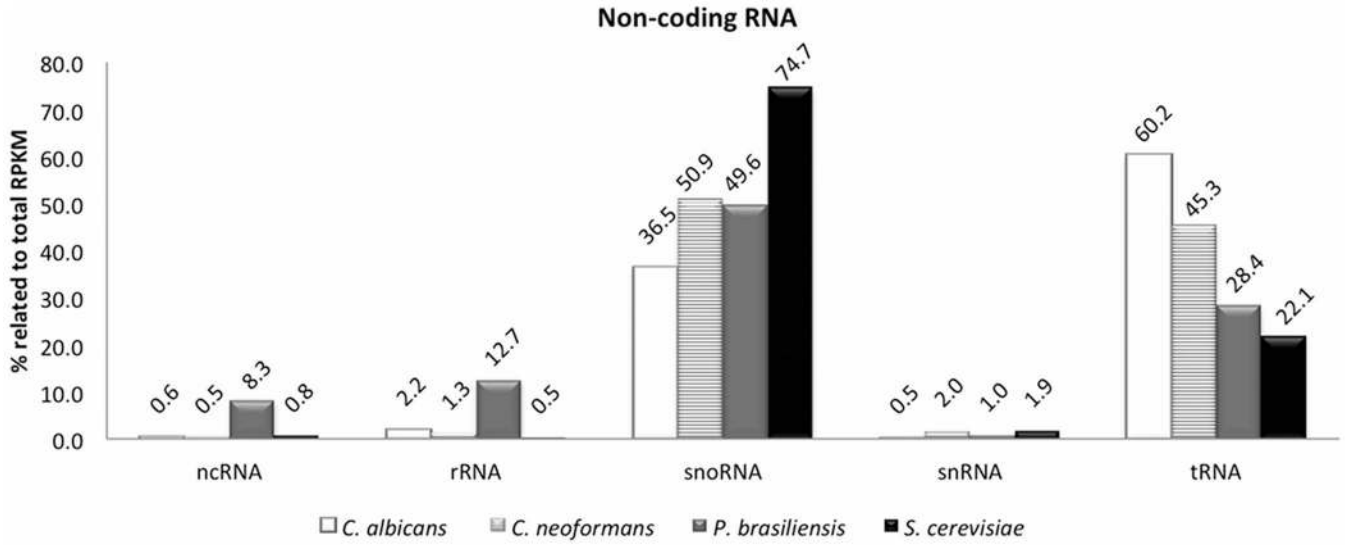

Figure 4 | Distribution of noncoding RNA species (other than miRNA-like species) in fungal EVs. The percentages of each RNA species indicated on the x-axis are expressed relative to total RKPM. Pb, *P. brasiliensis*; Cn, *C. neoformans*; Ca, *C. albicans*; Sc, *S. cerevisiae*.

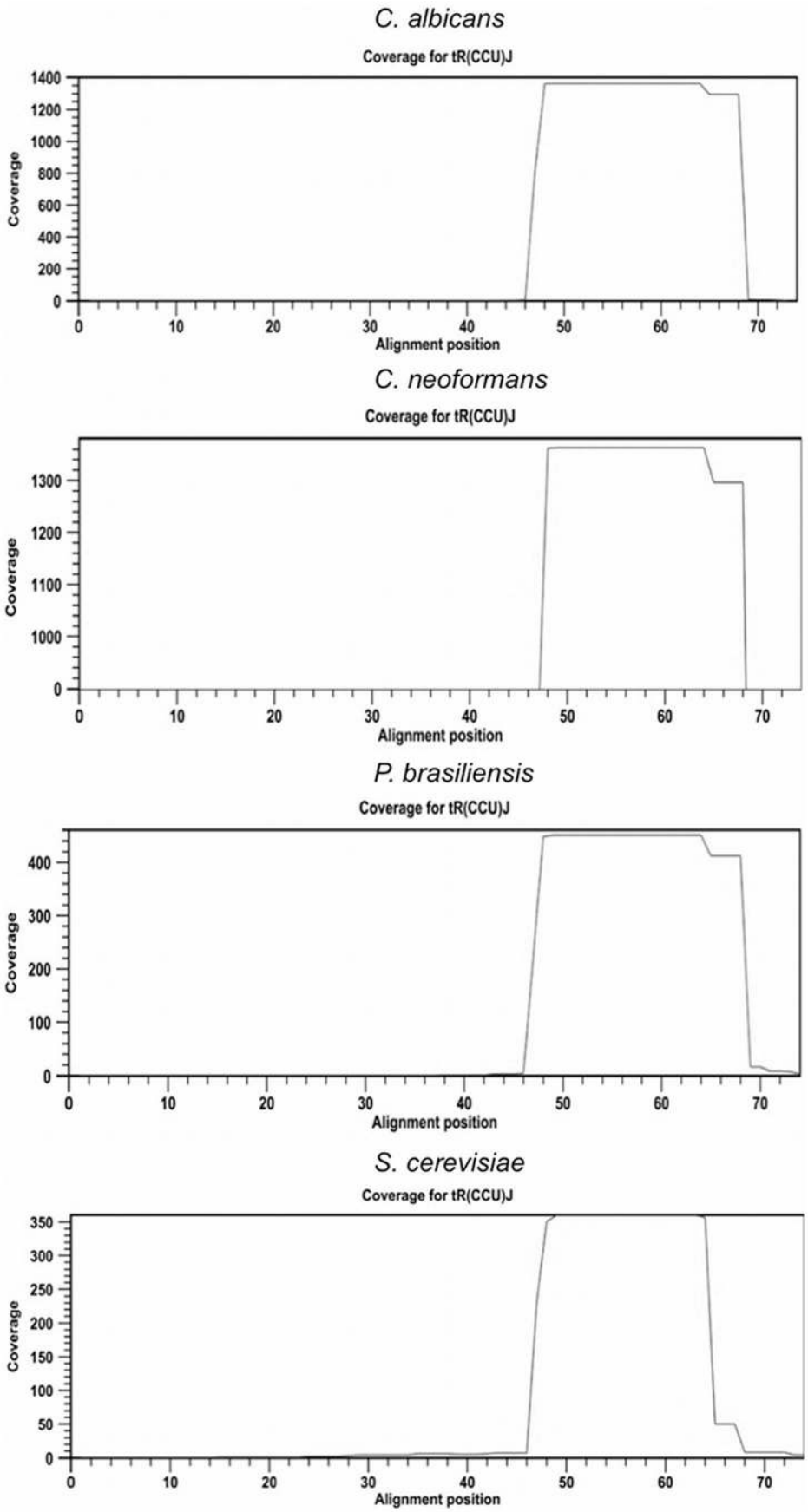

Figure 5 | Schematic graphs of reads aligning specifically with the 3′ end of the arginine tRNA(CCU)J identified in EVs from *P. brasiliensis*, *C. neoformans*, *C. albicans*, and *S. cerevisiae*. Coverage is indicated on the *y*-axis and alignment position is shown on the *x*-axis.

Table 4 | mRNA sequences identified in P. brasiliensis, C. neoformans, C. albicans, and S. cerevisiae EVs

Species	Feature ID	Product	Means normalized RPKM
C. albicans	orf19.6834.10	Ortholog of *S. cerevisiae* Tar1p	415068.82
	orf19.1742	Hydroxymethylbilane synthase	12255.92
	orf19.6140	Protein with similarity to ferric reductases	9716.90
	orf19.6336	Putative GPI-anchored adhesin-like protein	1279.89
	orf19.5628	Mitochondrial dicarboxylate transporter	1784.62
	orf19.3540	Putative nucleolar DEAD-box RNA helicase	1058.57
	orf19.101	Protein required for alkaline pH response	1389.34
	orf19.5284	CAWG_01866	983.61
	orf19.7073	YCL002C	947.91
	orf19.1661	RNA helicase activity, translational termination	815.58
C. neoformans	CNAG_06164	Hypothetical protein	10215.06
	CNAG_03379	N-acetyltransferase 5	9142.90
	CNAG_03382	Hypothetical protein	6224.73
	CNAG_06220	Allergen	4180.13
	CNAG_02724	Hypothetical protein	3374.93
	CNAG_06101	Eukaryotic ADP/ATP carrier	2070.80
	CNAG_03667	Hypothetical protein	3112.63
	CNAG_01052	Hypothetical protein	1875.03
	CNAG_01743	Hypothetical protein	1880.59
	CNAG_06646	ypt interacting protein	1574.72
P. brasiliensis	PADG_06364	Hypothetical protein	160376.61
	PADG_08536	Conserved hypothetical protein	141933.83
	PADG_03535	Nucleotide-binding protein	37239.82
	PADG_07966	ser/Thr protein phosphatase family protein	15709.62
	PADG_02959	Predicted protein	4210.27
	PADG_08534	Hypothetical protein	5423.77
	PADG_01121	Conserved hypothetical protein	4743.93
	PADG_06655	Coatomer subunit delta	3029.63
	PADG_01377	Hypothetical protein	2336.68
	PADG_08533	Conserved hypothetical protein	1293.54
S. cerevisiae	BAS1	Myb-related transcription fator	2577.53
	CLB3	B-type cyclin involved in cell cycle progression	1074.90
	PRM4	Pheromone-regulated protein involved in mating	932.26
	DAD2	Essential subunit of the Dam1 complex	886.83
	ATG8	Component of autophagosomes and Cvt vesicles	346.86
	TAO3	Component of the RAM signaling network	340.95
	YJU2	Essential protein required for pre-mRNA splicing	278.14
	ASH1	Zinc-finger inhibitor of HO transcription	272.97
	PAN1	Part of actin cytoskeleton-regulatory complex	219.88
	YKR023W	Putative protein of unknown function	199.01

(2.09-fold). The EVs of *C. neoformans* were enriched in mRNAs corresponding to the transport (3.61-fold), cytoskeleton organization (3.06-fold), signal transduction (2.37-fold), and vesicle-mediated transport (1.94-fold) categories (Table 5).

We then compared the RNA content of extracellular vesicles with that of other vesicles from the species studied. The analysis was performed with OrthoMCL software[86], which uses the Markov Clustering (MCL) algorithm designed to group orthologous sequences on a genome-wide scale. It identifies molecules orthologous in different species, and functionally redundant or "recent", paralogs within species. Most of the RNAs identified were species-specific: 70% were exclusive to *S. cerevisiae*, 89% to *P. brasiliensis*, 91% to *C. neoformans*, and 92% to *C. albicans* (Fig. 7). None of the mRNA sequences were common to all four fungi, but we identified orthologs in two or three species. The largest numbers of orthologs were found in *C. neoformans* and *S. cerevisiae* (16) and in *C. neoformans* and *C. albicans* (11 RNAs). The small numbers of orthologs common to several species may reflect the characteristics of each species and of the RNA cargo, which plays a specific role in each fungus. This result differs from the observations made during proteomic comparisons of the vesicles, for which a core set of proteins was found to be common to different fungal species[3].

Conclusions. We characterized EVs as biological carriers of fungal RNA. The implications of these findings for fungal physiology and pathogenesis remain unclear, but the presence of RNA in fungal EVs is consistent with the hypothesis that the vesicle-mediated export of nucleic acids interferes with gene expression in host and fungal cells. The presence of different RNA classes in fungal EVs opens up new possibilities for investigating the ways in which fungal cells communicate and respond to external stimuli. Our results suggest that the RNA exported by fungi may interfere with the physiology of host tissues.

Methods

Fungal strains and growth conditions. The P. brasiliensis isolate used in our study was Pb18, which was recovered from the lungs of BALB/c mice after experimental infection. Eight-week-old male Balb/c were obtained from the Center for Development of Experimental Models (CEDEME), at Universidade Federal de São Paulo (UNIFESP). Animals were kept in ventilated isolators at 22 ± 2 °C and 55 ± 10% humidity. All animal manipulations were made in compliance with the protocols approved by Federal University of São Paulo Ethics Committee for Animal Experimentation (project approval number 366/07). Pb18 cells were maintained in the yeast phase at 36 °C, in solid, modified YPD medium (0.5% yeast extract, 0.5% casein peptone, 1.5% glucose, pH 6.5). Yeast cells were transferred from seven-day-old slant cultures to Erlenmeyer flasks containing Ham's F12 medium (Invitrogen) supplemented with 1.5% glucose, in which they were cultured for four days at 36 °C, with shaking (pre-inoculum). Cells from four pre-inocula were then collected by gravitational sedimentation. As much supernatant as possible was removed and the cells were used to inoculate fresh medium (500 ml). They were cultured at high density for another 48 h, for vesicle purification. The *C. neoformans* isolate was the standard strain H99 (serotype A), which was maintained at 30 °C in Sabouraud dextrose plates (1% dextrose, 4% peptone). Yeast cells recovered from the plates were

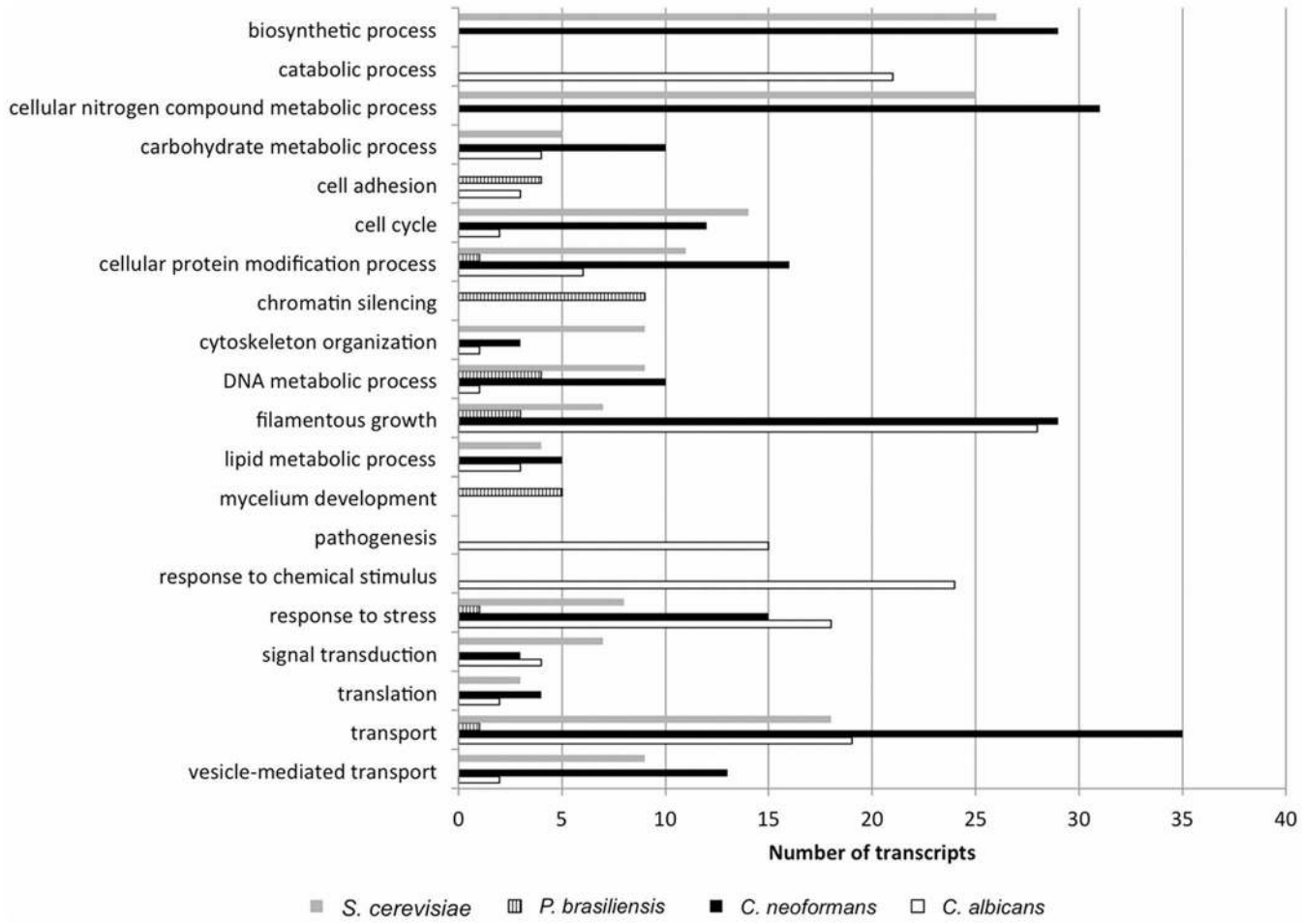

Figure 6 | Gene Ontology (GO) function profile of proteins corresponding to the high-coverage RNA sequences identified in the sRNA-enriched fractions isolated from EVs from *P. brasiliensis*, *C. neoformans*, *C. albicans*, and *S. cerevisiae*. The number of hits identified for each term is indicated on the *x*-axis.

used to inoculate minimal medium composed of dextrose (15 mM), $MgSO_4$ (10 mM), KH_2PO_4 (29.4 mM), glycine (13 mM), and thiamine-HCl (3 μM), and were cultured for three days at 30 °C, with shaking. *S. cerevisiae* (strain SEY6210) cells were maintained at 25 °C for 24 h, on Sabouraud dextrose plates. For EV isolation, yeast cells were transferred to Sabouraud dextrose broth and cultured for an additional 24 h at 25 °C, with shaking. Strain 11 of *C. albicans* was isolated from a

Table 5 | Gene Ontology (GO) function profile from *P. brasiliensis*, *C. neoformans*, *C. albicans*, and *S. cerevisiae* EVs. * p-value < 0.05

Sp	GO – Cellular Process	EVs/genome ratio*
C. neoformans	Growth	3.61
	Cytoskeleton organization	3.06
	Signal transduction	2.37
	Homeostatic process	1.97
	Vesicle-mediated transport	1.94
	Cell cycle	1.9
	Protein targeting	1.69
	Reproduction	1.57
	Cellular protein modification	1.35
C. albicans	Vesicle-mediated transport	2.43
	Catabolic process	2.1
	Transport	2.09
	Cellular protein modification	1.7
	Cellular component assembly	1.63
	Cell cycle	1.41
S. cerevisiae	Cellular protein modification	2.18
	Small molecule metabolic process	1.82
	Ribosome biogenesis	1.73
	Transport	1.61
	Response to stress	1.54
	Cellular nitrogen compound metabolic process	1.41

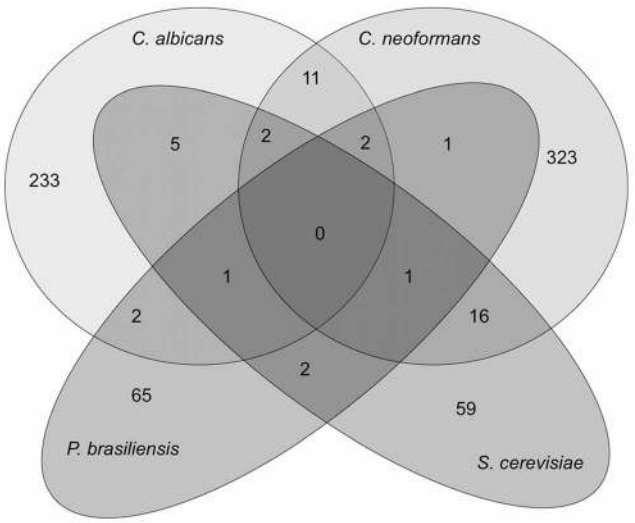

Figure 7 | Venn diagram of orthologous RNA sequences identified in the sRNA-enriched fractions isolated from the extracellular vesicles of *P. brasiliensis* (*n* = 73), *C. neoformans* (*n* = 353), *C. albicans* (*n* = 253), and *S. cerevisiae* (*n* = 84).

male patient[87] and kindly provided by Dr. Dornelas from the Institute of Hematology Arthur Siqueira Cavalcanti (Rio de Janeiro, Brazil). *C. albicans* cells were maintained at 36°C on Sabouraud dextrose plates. For EV isolation, yeast cells were grown in Sabouraud dextrose broth, with shaking, at 36°C for 48 h.

Vesicle isolation. EVs were isolated from fungal culture supernatants, as previously described[10,16]. Briefly, cell-free culture supernatants were recovered by centrifugation at 4,000 × *g* for 15 minutes at 4°C and the resulting supernatants were recentrifuged at 15,000 × *g* for 30 minutes, to remove smaller debris. The final supernatants were concentrated by a factor of 20 with an Amicon ultrafiltration system (100-kDa cutoff, Millipore). Concentrated supernatants were centrifuged at 15,000 × *g* for 30 minutes, to ensure the removal of aggregates, and the resulting supernatant was then ultracentrifuged at 100,000 × *g* for 1 h to precipitate vesicles. Vesicle pellets were washed once in phosphate-buffered saline (PBS), and the final pellets were suspended in PBS and lyophilized for RNA isolation.

sRNA isolation. RNA was isolated with the RNeasy mini kit (Qiagen), and was then treated with the RNeasy MinElute Cleanup Kit (Qiagen) according to the manufacturer's protocol, to obtain small RNA-enriched fractions. We used an Agilent 2100 Bioanalyzer (Agilent Technologies) to detect small RNA (sRNA) molecules. For the confirmation of sRNA extraction, some extracellular vesicle preparations were treated with 30 U DNase I (Qiagen) and characterized with the Bioanalyzer. We checked that the RNA was confined within the extracellular vesicles, as previously described[22]. We added 5 μg cellular RNA or no cellular RNA to the Pb18 preparation, which was then treated with 0.4 μg μl^{-1} RNase (Promega) for 10 minutes at 37 °C. RNase was inactivated by incubation for 10 minutes at 65 °C, after which, RNA was extracted immediately.

RNA sequencing. We used 100 ng of purified sRNA for RNA-seq from three independent biological replicates. The RNA-seq was performed in a SOLiD 4 platform using RNA-Seq kit according to the manufacturer's recommendations.

***In silico* data analysis.** The sequencing data obtained were analyzed with CLC Genomics Workbench© v 5.5.1. The reads were trimmed on the basis of quality, with a threshold Phred score of 15. The reference genomes used for mapping were obtained from the NCBI database (*C. neoformans* - GCA_000149245.3, *C. albicans* - GCA_000149445.2, *P. brasiliensis* - GCA_000150735.1 and *S. cerevisiae* - GCA_000146045.2). The alignment was performed as follows: additional 100-base upstream and downstream sequences; minimum number of reads, 10; maximum number of mismatches, 2; nonspecific match limit, −2 and minimum length fraction of 0.9 for the genome mapping and 1.0 for the miRNA mapping. The minimum similarity of the reads mapped on the reference genome was 80%. Only uniquely mapped reads were considered in the analysis. The libraries were normalized per million and the expression values for the transcripts are presented in RPKM (Reads Per Kilobase per Million).

Quantitative PCR (qPCR). DNA and RNA were extracted from *P. brasiliensis* yeast cells recovered from EV preparations, as previously described[88]. Due to the absence of control genes in EV preparations, a standard curve based on amplified DNA fragments was constructed, for rough quantification of the target sequences in *P. brasiliensis* RNA isolated from yeast cells and EVs. Sequences were initially amplified from isolated genomic DNA with primers for PADG_00645 (F:5′-GGATCTGAAAGGCACCCGAA-3′ and R:5′-ACCCATACGCTCTACCCCTT-3′) and PADG_00901 (R:5′-CCGATGCCAGCACTACTACC-3′; F:5′-CCATGACATCGACACCGGAA-3′). The reaction mixture (50 μl) contained 1U of *Taq* High-Fidelity Platinum polymerase (Invitrogen), 2 mM $MgSO_4$, 0.4 mM of each primer and 0.2 mM of dNTP in High-Fidelity PCR buffer. Amplifications were performed as follows: 5 minutes at 94 °C, followed by 35 cycles of 94 °C for 1 minutes, 60 °C for 1 minute and 70 °C for 1 minute, followed by an extension phase of 7 minutes at 72°C. The final product was purified with gel electrophoresis and the QIAEX II Gel Extraction kit (Qiagen) after the excision of amplicons from the 2.5% agarose gel. Amounts were estimated in a Nanodrop device and the number of molecules was estimated with a tool available from http://www.sciencelauncher.com/mwcalc.html site. We carried out qPCR with the Fast SYBR® Green Master Mix (Applied Biosystems), according to the manufacturer's instructions, in a 7500 Fast Real-Time PCR System (Applied Biosystems). Cycling conditions were as follows: 2 minutes at 50 °C, 1 minute at 95 °C, followed by 40 cycles of 95 °C for 15 s and 60 °C for 1 s. An additional cycle of 95 °C for 15 s, 60 °C for 20 s, and 95 °C for 15 s was performed, to determine the dissociation curve at the end of the reaction. The standard curve for absolute quantification from genomic DNA, based on decreasing known numbers of copies (10^6, 10^5, 10^4, 10^3 and 10^2 theoretical copies), was constructed in parallel, from total cell and EV RNA reactions. Measurements were made in triplicate.

Data access. The data have been submitted to the Sequence Read Archive (SRA) database under study accession number (SRA: SRP022849).

1. Ludwig, A. K. & Giebel, B. Exosomes: small vesicles participating in intercellular communication. *Int J Biochem Cell Biol* **44**, 11–15 (2012).
2. Rodrigues, M. L. *et al.* Vesicular transport systems in fungi. *Future Microbiol* **6**, 1371–1381 (2011).
3. Vallejo, M. C. *et al.* Vesicle and vesicle-free extracellular proteome of *Paracoccidioides brasiliensis*: comparative analysis with other pathogenic fungi. *J Proteome Res* **11**, 1676–1685 (2012).
4. Oliveira, D. L. *et al.* Characterization of yeast extracellular vesicles: evidence for the participation of different pathways of cellular traffic in vesicle biogenesis. *PLoS One* **5**, e11113 (2010).
5. Panepinto, J. *et al.* Sec 6-dependent sorting of fungal extracellular exosomes and laccase of *Cryptococcus neoformans*. *Mol Microbiol* **71**, 1165–1176 (2009).
6. Nicola, A. M., Frases, S. & Casadevall, A. Lipophilic dye staining of *Cryptococcus neoformans* extracellular vesicles and capsule. *Eukaryot Cell* **8**, 1373–1380 (2009).
7. Oliveira, D. L. *et al.* *Cryptococcus neoformans* cryoultramicrotomy and vesicle fractionation reveals an intimate association between membrane lipids and glucuronoxylomannan. *Fungal Genet Biol* **46**, 956–963 (2009).
8. Eisenman, H. C., Frases, S., Nicola, A. M., Rodrigues, M. L. & Casadevall A. Vesicle-associated melanization in *Cryptococcus neoformans*. *Microbiology* **155**, 3860–3867 (2009).
9. Rodrigues, M. L. *et al.* Extracellular vesicles produced by *Cryptococcus neoformans* contain protein components associated with virulence. *Eukaryot Cell* **7**, 58–67 (2008).
10. Rodrigues, M. L. *et al.* Vesicular polysaccharide export in *Cryptococcus neoformans* is a eukaryotic solution to the problem of fungal trans-cell wall transport. *Eukaryot Cell* **6**, 48–59 (2007).
11. Tefsen, B. *et al.* Deletion of the CAP10 gene of *Cryptococcus neoformans* results in a pleiotropic phenotype with changes in expression of virulence factors. *Res Microbiol* **165**, 399–410 (2014).
12. Giardina, B. J., Stein, K. & Chiang, H. L. The endocytosis gene END3 is essential for the glucose-induced rapid decline of small vesicles in the extracellular fraction in *Saccharomyces cerevisiae*. *J Extracell Vesicles* **3**, 23497 (2014).
13. Giardina, B. J., Stanley, B. A. & Chiang, H. L. Glucose induces rapid changes in the secretome of *Saccharomyces cerevisiae*. *Proteome Sci* **12**, 9 (2014).
14. Silva, B. M. *et al.* Characterization of Alternaria infectoria extracellular vesicles. *Med Mycol* **52**, 202–210 (2014).
15. Vallejo, M. C. *et al.* Lipidomic analysis of extracellular vesicles from the pathogenic phase of *Paracoccididoides brasiliensis*. *PLoS One* **7**, e39463 (2012).
16. Vallejo, M. C. *et al.* The pathogenic fungus *Paracoccididoides brasiliensis* exports extracellular vesicles containing highly immunogenic alpha-galactosyl epitopes. *Eukaryot Cell* **10**, 343–351 (2011).
17. Rizzo, J. *et al.* Role of the Apt1 protein in polysaccharide secretion by *Cryptococcus neoformans*. *Eukaryot Cell* **13**, 715–726 (2014).
18. Albuquerque, P. C. *et al.* Vesicular transport in *Histoplasma capsulatum*: an effective mechanism for trans-cell wall transfer of proteins and lipids in ascomycetes. *Cell Microbiol* **10**, 1695–1710 (2008).
19. Rodrigues, M. L., Franzen, A. J., Nimrichter, L. & Miranda, K. Vesicular mechanisms of traffic of fungal molecules to the extracellular space. *Curr Opin Microbiol* **16**, 414–420 (2013).
20. Rodrigues, M. L., Nakayasu, E. S., Almeida, I. C. & Nimrichter, L. The impact of proteomics on the understanding of functions and biogenesis of fungal extracellular vesicles. *J Proteomics* **97**, 177–186 (2014).
21. Ratajczak, J., Wysoczynski, M., Hayek, F., Janowska-Wieczorek, A. & Ratajczak, M. Z. Membrane-derived microvesicles: important and underappreciated mediators of cell-to-cell communication. *Leukemia* **20**, 1487–1495 (2006).

22. Valadi, H. *et al.* Exosome-mediated transfer of mRNAs and microRNAs is a novel mechanism of genetic exchange between cells. *Nat Cell Biol* **9**, 654–659 (2007).
23. Pegtel, D. M. *et al.* Functional delivery of viral miRNAs via exosomes. *Proc Natl Acad Sci USA* **107**, 6328–6333 (2010).
24. Garcia-Silva, M. R. *et al.* Extracellular vesicles shed by *Trypanosoma cruzi* are linked to small RNA pathways, life cycle regulation, and susceptibility to infection of mammalian cells. *Parasitol Res* **113**, 285–304 (2014).
25. Garcia-Silva, M. R. *et al.* Gene expression changes induced by *Trypanosoma cruzi* shed microvesicles in mammalian host cells: relevance of tRNA-derived halves. *Biomed Res Int* **2014**, 305239 (2014).
26. Wei, W. *et al.* Genome sequencing and comparative analysis of *Saccharomyces cerevisiae* strain YJM789. *Proc Natl Acad Sci USA* **104**, 12825–12830 (2007).
27. Jones, T. *et al.* The diploid genome sequence of *Candida albicans*. *Proc Natl Acad Sci USA* **101**, 7329–7334 (2004).
28. Zhang, Y. *et al.* Secreted monocytic miR-150 enhances targeted endothelial cell migration. *Mol Cell* **39**, 133–144 (2010).
29. Kosaka, N. *et al.* Secretory mechanisms and intercellular transfer of microRNAs in living cells. *J Biol Chem* **285**, 17442–17452 (2010).
30. Baggerly, K. A., Deng, L., Morris, J. S. & Aldaz, C. M. Differential expression in SAGE: accounting for normal between-library variation. *Bioinformatics* **19**, 1477–1483 (2013).
31. Jin, H., Kim, V. N. & Hyun, S. Conserved microRNA miR-8 controls body size in response to steroid signaling in Drosophila. *Genes Dev* **26**, 1427–1432 (2012).
32. Kennell, J. A., Gerin, I., MacDougald, O. A. & Cadigan, K. M. The microRNA miR-8 is a conserved negative regulator of Wnt signaling. *Proc Natl Acad Sci USA* **105**, 15417–15422 (2008).
33. Choi, I. K. & Hyun, S. Conserved microRNA miR-8 in fat body regulates innate immune homeostasis in Drosophila. *Dev Comp Immunol* **37**, 50–54 (2012).
34. Flynt, A. S. & Patton, J. G. Crosstalk between planar cell polarity signaling and miR-8 control of NHERF1-mediated actin reorganization. *Cell Cycle* **9**, 235–237 (2010).
35. Vallejo, D. M., Caparros, E. & Dominguez, M. Targeting Notch signalling by the conserved miR-8/200 microRNA family in development and cancer cells. *EMBO J* **30**, 756–769 (2011).
36. Jung, J. H., Seo, P. J., Kang, S. K. & Park, C. M. miR172 signals are incorporated into the miR156 signaling pathway at the SPL3/4/5 genes in Arabidopsis developmental transitions. *Plant Mol Biol* **76**, 35–45 (2011).
37. Jung, J. H. & Park, C. M. MIR166/165 genes exhibit dynamic expression patterns in regulating shoot apical meristem and floral development in Arabidopsis. *Planta* **225**, 1327–1338 (2007).
38. Ong, S. S. & Wickneswari, R. Characterization of microRNAs expressed during secondary wall biosynthesis in Acacia mangium. *PLoS One* **7**, e49662 (2012).
39. Sun, Y. M., Lin, K. Y. & Chen, Y. Q. Diverse functions of miR-125 family in different cell contexts. *J Hematol Oncol* **6**, 6 (2013).
40. Bousquet, M., Nguyen, D., Chen, C., Shields, L. & Lodish, H. F. MicroRNA-125b transforms myeloid cell lines by repressing multiple mRNA. *Haematologica* **97**, 1713–1721 (2012).
41. Suh, E. J. *et al.* A microRNA network regulates proliferative timing and extracellular matrix synthesis during cellular quiescence in fibroblasts. *Genome Biol* **13**, R121 (2012).
42. Bi, Q. *et al.* Ectopic expression of MiR-125a inhibits the proliferation and metastasis of hepatocellular carcinoma by targeting MMP11 and VEGF. *PLoS One* **7**, e40169 (2012).
43. Xu, Y., Zhou, B., Wu, D., Yin, Z. & Luo, D. Baicalin modulates microRNA expression in UVB irradiated mouse skin. *J Biomed Res* **26**, 125–134 (2012).
44. Ge, Y., Sun, Y. & Chen, J. IGF-II is regulated by microRNA-125b in skeletal myogenesis. *J Cell Biol* **192**, 69–81 (2011).
45. Wang, G., Jiang, B., Jia, C., Chai, B. & Liang, A. MicroRNA 125 represses nonsense-mediated mRNA decay by regulating SMG1 expression. *Biochem Biophys Res Commun* **435**, 16–20 (2013).
46. Gururajan, M. *et al.* MicroRNA 125b inhibition of B cell differentiation in germinal centers. *Int Immunol* **22**, 583–592 (2010).
47. Willimott, S. & Wagner, S. D. miR-125b and miR-155 contribute to BCL2 repression and proliferation in response to CD40 ligand (CD154) in human leukemic B-cells. *J Biol Chem* **287**, 2608–2617 (2012).
48. Rajaram, M. V. *et al.* Mycobacterium tuberculosis lipomannan blocks TNF biosynthesis by regulating macrophage MAPK-activated protein kinase 2 (MK2) and microRNA miR-125b. *Proc Natl Acad Sci USA* **108**, 17408–17413 (2011).
49. Potenza, N. *et al.* Human microRNA hsa-miR-125a-5p interferes with expression of hepatitis B virus surface antigen. *Nucleic Acids Res* **39**, 5157–5163 (2011).
50. Dang, Y., Yang, Q., Xue, Z. & Liu, Y. RNA interference in fungi: pathways, functions, and applications. *Eukaryot Cell* **10**, 1148–1155 (2011).
51. Fulci, V. & Macino, G. Quelling. post-transcriptional gene silencing guided by small RNAs in *Neurospora crassa*. *Curr Opin Microbiol* **10**, 199–203 (2007).
52. Li, L., Chang, S. S. & Liu, Y. RNA interference pathways in filamentous fungi. *Cell Mol Life Sci* **67**, 3849–3863 (2010).
53. Drinnenberg, I. A. *et al.* RNAi in budding yeast. *Science* **326**, 544–550 (2009).
54. Jiang, N., Yang, Y., Janbon, G., Pan, J. & Zhu, X. Identification and functional demonstration of miRNAs in the fungus *Cryptococcus neoformans*. *PLoS One* **7**, e52734 (2012).
55. Wang, X. *et al.* Sex-induced silencing defends the genome of *Cryptococcus neoformans* via RNAi. *Genes Dev* **24**, 2566–2582 (2010).
56. Cifuentes, D. *et al.* A novel miRNA processing pathway independent of Dicer requires Argonaute2 catalytic activity. *Science* **328**, 1694–1698 (2010).
57. Bumgarner, S. L., Dowell, R. D., Grisafi, P., Gifford, D. K. & Fink, G. R. Toggle involving cis-interfering noncoding RNAs controls variegated gene expression in yeast. *Proc Natl Acad Sci USA* **106**, 18321–18326 (2009).
58. Fatica, A. & Bozzoni, I. Long non-coding RNAs: new players in cell differentiation and development. *Nat Rev Genet* **15**, 7–21 (2014).
59. Guttman, M. *et al.* Chromatin signature reveals over a thousand highly conserved large non-coding RNAs in mammals. *Nature* **458**, 223–227 (2009).
60. Bumgarner, S. L. *et al.* Single-cell analysis reveals that noncoding RNAs contribute to clonal heterogeneity by modulating transcription factor recruitment. *Mol Cell* **45**, 470–482 (2012).
61. Houser-Scott, F. *et al.* Interactions among the protein and RNA subunits of *Saccharomyces cerevisiae* nuclear RNase P. *Proc Natl Acad Sci USA* **99**, 2684–2689 (2002).
62. Marvin, M. C. *et al.* Accumulation of noncoding RNA due to an RNase P defect in *Saccharomyces cerevisiae*. *RNA* **17**, 1441–1450 (2011).
63. Xiao, S., Houser-Scott, F. & Engelke, D. R. Eukaryotic ribonuclease P: increased complexity to cope with the nuclear pre-tRNA pathway. *J Cell Physiol* **187**, 11–20 (2001).
64. Schmitt, M. E. & Clayton, D. A. Nuclear RNase MRP is required for correct processing of pre-5.8S rRNA in *Saccharomyces cerevisiae*. *Mol Cell Biol* **13**, 7935–7941 (1993).
65. Stohl, L. L. & Clayton, D. A. *Saccharomyces cerevisiae* contains an RNase MRP that cleaves at a conserved mitochondrial RNA sequence implicated in replication priming. *Mol Cell Biol* **12**, 2561–2569 (1992).
66. Gill, T., Aulds, J. & Schmitt, M. E. A specialized processing body that is temporally and asymmetrically regulated during the cell cycle in *Saccharomyces cerevisiae*. *J Cell Biol* **173**, 35–45 (2006).
67. Valadkhan, S. snRNAs as the catalysts of pre-mRNA splicing. *Curr Opin Chem Biol* **9**, 603–608 (2005).
68. Matera, A. G., Terns, R. M. & Terns, M. P. Non-coding RNAs: lessons from the small nuclear and small nucleolar RNAs. *Nat Rev Mol Cell Biol* **8**, 209–220 (2007).
69. Lafontaine, D. L. & Tollervey, D. Birth of the snoRNPs: the evolution of the modification-guide snoRNAs. *Trends Biochem Sci* **23**, 383–388 (1998).
70. Cavaillé, J. *et al.* Identification of brain-specific and imprinted small nucleolar RNA genes exhibiting an unusual genomic organization. *Proc Natl Acad Sci USA* **97**, 14311–14316 (2000).
71. Ganot, P., Bortolin, M. L. & Kiss T. Site-specific pseudouridine formation in preribosomal RNA is guided by small nucleolar RNAs. *Cell* **89**, 799–809 (1997).
72. Liang, B. *et al.* Structure of a functional ribonucleoprotein pseudouridine synthase bound to a substrate RNA. *Nat Struct Mol Biol* **16**, 740–746 (2009).
73. Tollervey, D. & Guthrie, C. Deletion of a yeast small nuclear RNA gene impairs growth. *EMBO J* **4**, 3873–3878 (1985).
74. Badis, G., Fromont-Racine, M. & Jacquier, A. A snoRNA that guides the two most conserved pseudouridine modifications within rRNA confers a growth advantage in yeast. *RNA* **9**, 771–779 (2003).
75. Esguerra, J., Warringer, J. & Blomberg, A. Functional importance of individual rRNA 2'-O-ribose methylations revealed by high-resolution phenotyping. *RNA* **14**, 649–656 (2008).
76. Garcia Silva, M. R. *et al.* Cloning, characterization and subcellular localization of a *Trypanosoma cruzi* argonaute protein defining a new subfamily distinctive of trypanosomatids. *Gene* **466**, 26–35 (2010).
77. Lee, Y. S., Shibata, Y., Malhotra, A. & Dutta, A. A novel class of small RNAs: tRNA-derived RNA fragments (tRFs). *Genes Dev* **23**, 2639–2649 (2009).
78. Kawakami, K. *et al.* A rare tRNA-Arg(CCU) that regulates Ty1 element ribosomal frameshifting is essential for Ty1 retrotransposition in *Saccharomyces cerevisiae*. *Genetics* **135**, 309–320 (1993).
79. Chan, P. P. & Lowe, T. M. GtRNAdb: a database of transfer RNA genes detected in genomic sequence. *Nucleic Acids Res* **37**, D93–97 (2009).
80. Mewes, H. W. *et al.* Overview of the yeast genome. *Nature* **387**, 7–65 (1997).
81. Felipe, M. S. *et al.* Functional genome of the human pathogenic fungus *Paracoccidiodoides brasiliensis*. *FEMS Immunol Med Microbiol* **45**, 369–381 (2005).
82. Loftus, B. J. *et al.* The genome of the basidiomycetous yeast and human pathogen *Cryptococcus neoformans*. *Science* **307**, 1321–1324 (2005).
83. Cosma, M. P. Daughter-specific repression of *Saccharomyces cerevisiae* HO: Ash1 is the commander. *EMBO Rep* **5**, 953–957 (2004).
84. Goldman, G. H. *et al.* Expressed sequence tag analysis of the human pathogen *Paracoccidiodoides brasiliensis* yeast phase: identification of putative homologues of *Candida albicans* virulence and pathogenicity genes. *Eukaryot Cell* **2**, 34–48 (2003).
85. Bruno, V. M. *et al.* Comprehensive annotation of the transcriptome of the human fungal pathogen *Candida albicans* using RNA-seq. *Genome Res* **20**, 1451–1458 (2010).
86. Li, L., Stoeckert, C. J. & Roos, D. S. OrthoMCL. identification of ortholog groups for eukaryotic genomes. *Genome Res* **13**, 2178–2189 (2003).
87. Braga-Silva, L. A. *et al.* Trailing end-point phenotype antibiotic-sensitive strains of *Candida albicans* produce different amounts of aspartyl peptidases. *Braz J Med Biol Res* **42**, 765–770 (2009).

88. Cisalpino, P. S. *et al*. Cloning, characterization, and epitope expression of the major diagnostic antigen of *Paracoccididoides brasiliensis*. *J Biol Chem* **271**, 4553–4560 (1996).

Acknowledgments

RP was supported by grants from the Brazilian agencies FAPESP, CNPq and CAPES. RPS received a scholarship from FAPESP. MLR was supported by grants from the Brazilian agencies FAPERJ, FAPESP, CAPES and CNPq and by the Instituto Nacional de Ciência e Tecnologia de Inovação em Doenças Negligenciadas (INCT-IDN). SG was supported by grants from the Brazilian agencies Fundação Araucária – PRONEX, CNPq and Papes-Fiocruz.

Author contributions

R.P.S., D.L.O., L.S.J. and G.V.C.: EV preparation, RNA fractionation, qPCR, RNA data analysis; LRA: RNA-seq and RNA data analysis; R.P.S., R.P., L.N., M.L.R., S.G. and L.R.A.: experimental design, analysis and interpretation of data. R.P.S., R.P. and L.R.A.: preparation of the manuscript. All authors discussed the results, wrote and approved the final manuscript.

Additional information

Supplementary information accompanies this paper at http://www.nature.com/scientificreports

Competing financial interests: The authors declare no competing financial interests.

How to cite this article: da Silva, R.P. *et al*. Extracellular vesicle-mediated export of fungal RNA. *Sci. Rep.* **5**, 7763; DOI:10.1038/srep07763 (2015).